

## Self-Induced Zeeman Coherences in a Paul Trap

H. Harde, H. Lehmitz<sup>\*</sup>, J. Hattendorf-Ledwoch<sup>\*\*</sup>, and R. Blatt<sup>\*\*\*</sup>

Universität der Bundeswehr Hamburg, Fachbereich Elektrotechnik  
Holstenhofweg 85, W-2000 Hamburg 70, Fed. Rep. Germany, Fax: 40-653 0413

Received 18 April 1991/Accepted 25 June 1991

**Abstract.** A new method for the measurement of motional frequencies and amplitudes of stored ions in a radio-frequency trap is presented. Ions oscillating in the trap potential and additionally subjected to a small magnetic field, undergo sublevel transitions between adjacent Zeeman states when their motional frequency is identical with the Larmor frequency in the applied magnetic field. These transitions can be sensitively detected by means of an optical pumping scheme. As they are related to a coherent superposition of adjacent states and originate from the inherent motion of the ions in a slightly inhomogeneous magnetic field, this phenomenon is termed self-induced Zeeman coherence.

**PACS:** 32.80.Pj, 35.80.+s

Much attention is currently being devoted to the confinement of ions in Penning and Paul traps. Experiments with stored ions have made possible new kinds of fundamental and high-accuracy measurements. With single trapped ions the phenomenon of quantum jumps has been demonstrated [1–3] and optically cooled ions have been found to form a crystal structure [4, 5]. As ions can be stored for long periods without perturbations, transit-time broadening and collisional effects can largely be eliminated. Therefore trapped ions with well-defined rf or optical transitions are widely discussed as candidates for new frequency standards in both the microwave and the optical region [6–12].

For these applications, in general, the motion of trapped ions limits the ultimate frequency resolution. While Doppler broadening of an atomic transition can be avoided by confining the ions within a cloud smaller than the transition wavelength [13], systematic line shifts caused by the second-order Doppler effect still have to be considered. Single ions would satisfy the most stringent conditions for high precision measurements, as their energy can be efficiently reduced by optical sideband

cooling [14, 15]. But such experiments suffer from poor signal-to-noise ratios. On the other hand it has turned out that sufficient cooling of larger ion clouds in an rf trap is not possible due to rf-heating by the time-dependent trapping potential. For corrections of line shifts and the development of improved ion cooling techniques it is therefore of interest to obtain a knowledge of the kinetic energy and dynamics of the ions. The particle motion can be described as an approximate harmonic oscillation with the secular frequency (macromotion), additionally modulated by the micromotion originating from the driving frequency of the rf-field. These oscillations have been observed as sidebands of an atomic transition [16, 17, 10] and were used to determine the kinetic energy of the ions in the trap [18].

In this paper we describe a new method for the measurement of motional frequencies and amplitudes of stored ions by taking advantage of a direct resonance of an ion oscillation with an atomic sublevel splitting. In a small magnetic field a transition between adjacent Zeeman states can be observed and sensitively detected via optical transitions when the Larmor frequency is identical with an oscillation frequency of the ions. This phenomenon is interpreted as motional- or self-induced Zeeman coherence caused by the oscillations of the ions in a slightly inhomogeneous magnetic field.

A description of the experimental set-up is given in Sect. 1, while the measurements are discussed in Sect. 2. A theoretical model of the self-induced Zeeman coherences

<sup>\*</sup> Present address: Wild Leitz Systemtechnik GmbH, Ernst-Leitz-Strasse, W-6330 Wetzlar, Fed. Rep. Germany

<sup>\*\*</sup> Present address: Hoedtk & Boës KG, Postfach, W-2080 Pinneberg, Fed. Rep. Germany

<sup>\*\*\*</sup> Permanent address: Universität Hamburg, I. Institut für Experimentalphysik, Jungiusstrasse 9, W-2000 Hamburg 36, Fed. Rep. Germany

is presented in Sect. 3. Finally, we discuss the applications of this phenomenon for the measurement of trap parameters and the characterization of the ion motion.

## 1. Experimental Set-Up

For our experiments we used an rf ion trap by which up to  $10^7$  ions can be stored (see, for example, [19]). The experimental set-up is shown in Fig. 1. The investigations were performed with Yb available as natural abundance and as 95% enriched isotope  $^{173}\text{Yb}$ . The ions are produced by electron bombardment of atomic Yb evaporated by a hot wire in one of the trap's end caps. To measure the influence of buffer gases on the ion motion, the vacuum chamber containing the ion trap can be backfilled with rare gases to the order of 0.1 Pa.

The ions are optically excited by frequency-doubled laser light from a synchronously pumped mode-locked Rhodamine 700 dye laser which delivers pulses of 10 ps duration with bandwidth of 80 GHz and an average power of 1 mW at the second harmonic. The wavelength is tuned to the  $D_1$  resonance line of  $\text{Yb}^+$  at  $\lambda = 369.42$  nm (Fig. 2). While the infrared radiation behind the frequency doubler ( $\text{LiIO}_3$  crystal) is blocked by a filter, the UV-output passes a  $\lambda/4$  plate to obtain circularly polarized light necessary for the experiments.

Additionally, the ions are subjected to a small magnetic field with the field direction parallel to the propagation axis of the laser light ( $z$ -direction). This field is provided by Helmholtz coils and can be varied continuously from  $-50 \mu\text{T}$  up to  $250 \mu\text{T}$ . The earth's magnetic field is compensated in three dimensions by additional Helmholtz coils.

Fluorescence light from the excited ions is detected by a photomultiplier perpendicular to the laser beam through one of the trap electrodes which is formed out of transparent mesh. The output signal of the photomultiplier is stored as a function of the magnetic field by a computer.

In a previous publication [20] we described the phenomenon of completely vanishing fluorescence after resonant excitation of  $\text{Yb}^+$  ions caused by population trapping in the highly metastable  $4f^{13}6s^2F_{7/2}$ -state. However, under the experimental conditions realized here, the spectral width of the laser pulses simultaneously covers the resonance line as well as a transition from the metastable to a still higher lying level. Thus, the deadlock of population trapping in the  $^2F_{7/2}$  state is overcome and enough ions can be transferred back to the ground state to ensure a further excitation for continuous observation.

## 2. Measurements and Interpretation

Excitation of the ions with, e.g., left-handed polarized light and in a magnetic field parallel to the propagation axis of the laser beam induces  $\sigma^+$ -transitions as illustrated in Fig. 2 by a level scheme for the even isotopes with zero nuclear magnetic spin. Due to optical pumping the ions accumulate in the Zeeman sublevel with largest mag-

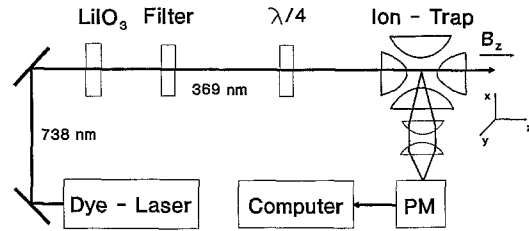


Fig. 1. Experimental set-up for measuring self-induced Zeeman coherences

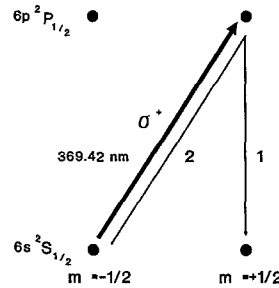


Fig. 2. Optical pumping scheme for a spin 1/2 particle

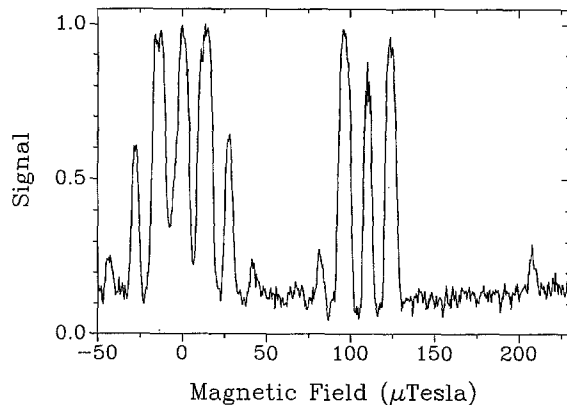


Fig. 3. Fluorescence intensity as a function of the longitudinal magnetic field representing the motional spectrum of  $^{173}\text{Yb}$  ions

netic quantum number,  $m = |J|$  (for the odd isotopes:  $m = |F|$ ), from which no further excitation is possible. Therefore reduced fluorescence is observed. Only at zero magnetic field when all sublevels are degenerate, is there no resulting polarization of the ground state population and maximum fluorescence is found.

A measurement of the fluorescence as a function of the longitudinal magnetic field with the enriched isotope sample of  $^{173}\text{Yb}$  is shown in Fig. 3. Contrary to usual optical pumping experiments, however, some additional strong peaks besides zero magnetic field show up, which obviously pertain to the confinement of the ions in the trap. These resonances appear at field strengths for which the level splitting between adjacent Zeeman substates is identical with the expected oscillation frequencies of the ions in the trap.

In a small magnetic field  $B_z$  this splitting is given by the Larmor frequency  $\omega_L$ :

$$\omega_L = \frac{\mu_B}{\hbar} g B_z \quad (1)$$

where  $\mu_B$  is Bohr's magneton,  $\hbar$  Planck's constant/ $2\pi$  and  $g$  the gyromagnetic factor, which for the even isotopes is  $g_I = 2$ , for  $^{171}\text{Yb}$  with nuclear spin  $I = 1/2$ ,  $g_F = 1$  and for  $^{173}\text{Yb}$  with  $I = 5/2$ ,  $g_F = 1/3$ .

On the other hand the motion of single ions in an rf trap can be described for both cylindrical coordinates  $u = (r, x)$  of the trap as an oscillation of the form [21]

$$u(t) = A \left( 1 - \frac{q_u}{2} \cos \Omega t \right) \cos \left( \frac{\beta_u}{2} \Omega t - \phi \right) \quad (2)$$

governed by a pseudopotential which is formed by dc and ac voltages between ring and endcap electrodes with amplitudes  $U_{dc}$  and  $U_{ac}$  and a driving frequency  $\Omega$ . The rotational axis of the trap is assumed to point in  $x$ -direction. Equation (2) represents an oscillation with amplitude  $A$  and frequency  $\omega_u = \beta_u \Omega / 2$  (secular frequency) as the macromotion modulated by the micromotion originating from the driving field with frequency  $\Omega$ .  $\beta_u$  can be approximately expressed by the relation:

$$\beta_u = \sqrt{a_u + \frac{q_u^2}{2}} \quad (3)$$

with

$$a_x = -\frac{8eU_{dc}}{Mr_0^2\Omega^2} = -2a_r \quad \text{and} \quad q_x = -\frac{4eU_{ac}}{Mr_0^2\Omega^2} = -2q_r, \quad (4)$$

where  $M$  is the ion mass,  $r_0$  the radius of the ring electrode and  $e$  the electron charge. Under typical experimental conditions the spectrum of (2) consists of the low carrier frequency  $\omega_u$  and higher lying side-bands  $\Omega - \omega_u$  and  $\Omega + \omega_u$ .

For the measurement indicated in Fig. 3 we used an rf frequency  $\Omega/2\pi = 500$  kHz. The storage parameters (depending on the dc and ac voltages) were chosen in such a way that the axial and radial secular frequency were identical. The calculated value of  $\omega_u/2\pi = 60$  kHz coincides with the Larmor frequency of  $^{173}\text{Yb}$  ions at a magnetic field of  $B_z = \pm 14 \mu\text{Tesla}$  where the first resonances besides zero magnetic field are observed. The next two peaks at  $\pm 28 \mu\text{Tesla}$  and  $\pm 42 \mu\text{Tesla}$  are not expected from (2) but can also be attributed to the macromotion as their higher harmonics, indicating the degree of anharmonicity of this oscillation. The group of resonances at about  $110 \mu\text{Tesla}$  is caused by the micromotion at 500 kHz as well as sum and difference frequencies of micro- and macromotion. While the stronger, outlying components are in accordance with the spectrum of the single particle motion, the central peak is not expected from this model, but is explained in terms of classical radio-frequency transitions at the driving frequency which are induced by an rf magnetic field arising in the trap from the ac driving voltage.

In all these cases an increase of the fluorescence is an indication of sublevel transitions between Zeeman states, and these transitions are not only induced by externally supplied rf fields, but also by the motion of the ions. Therefore such motion can be sensitively observed if one of the spectral components of the motion coincides with the Larmor frequency.

Another example of a measured spectrum of stored  $^{173}\text{Yb}$  ions is shown in Fig. 4. In this case the secular

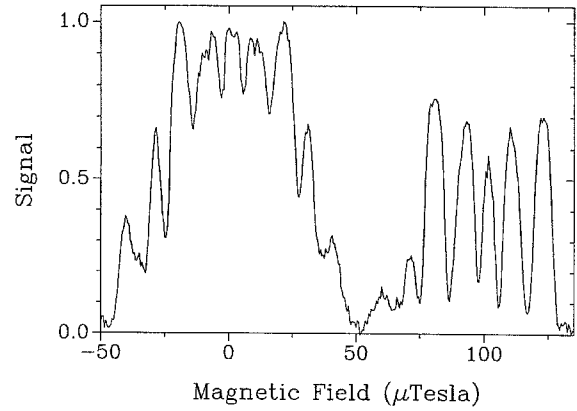


Fig. 4. Motional spectrum of  $^{173}\text{Yb}$  ions with nondegenerate secular frequencies in  $r$ - and  $x$ -directions

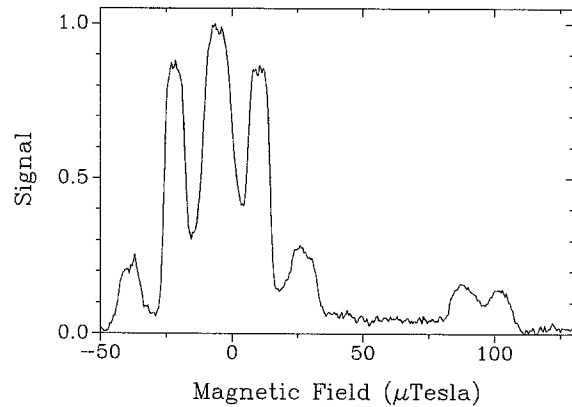


Fig. 5. Measurement of the motional spectrum using the natural isotopic abundance

frequencies in  $r$ - and  $x$ -direction were chosen to differ by a factor of two ( $U_{dc} = 0$  V) with  $\omega_r/2\pi = 48.5$  kHz and  $\omega_x/2\pi = 97$  kHz. The respective resonances can be identified at  $\pm 10.5 \mu\text{Tesla}$  and  $\pm 21 \mu\text{Tesla}$ . As the rf frequency with  $\Omega/2\pi = 460$  kHz was slightly reduced in comparison with the previous measurement, the group of resonances in the right part of Fig. 4, which contains the micromotion frequency and secular sidebands, is also shifted to smaller field values.

A measurement with the natural isotopic mixture of Yb is shown in Fig. 5. As the even isotopes have an abundance of 70%, they dominate in the observed structure and result in the strongest peaks besides zero at  $\pm 16.5 \mu\text{Tesla}$ . Due to the six times larger gyromagnetic factor of these isotopes compared with  $^{173}\text{Yb}$  ions, their resonances already appear at six times smaller magnetic fields, and hence the peaks at  $\pm 16.5 \mu\text{Tesla}$  have to be assigned to a group of unresolvable resonances caused by the micromotion at  $\Omega/2\pi = 460$  kHz and the sidebands with the macromotion. The peaks at  $\pm 33 \mu\text{Tesla}$  originate from  $^{171}\text{Yb}$  ions with  $g_F = 1$ , which are present in the isotopic mixture with an abundance of 14%. The structure at  $100 \mu\text{Tesla}$  is already known from the measurements with  $^{173}\text{Yb}$  having a concentration of 16%. The macromotion resonance of this isotope at about  $14 \mu\text{Tesla}$  is hidden by the peaks of the even isotopes.

### 3. Theoretical Model

The position of the observed resonances can be explained by sublevel transitions between adjacent Zeeman states with  $\Delta m = \pm 1$ , induced by the oscillation frequencies of the ions. But what is the physical origin of these transitions?

We assume that the ions are oscillating in a slightly inhomogeneous magnetic field with a position-dependent field component perpendicular to the  $z$ -axis. This component may result from imperfections and local variations of the fields applied in  $z$ -direction or from compensating the earth's magnetic field. It can be expressed by the position coordinate  $u = (r, x)$  of an ion in the trap and the field gradient  $\partial B_k / \partial u$  in  $k$ -direction ( $k = x, y$ ) by:

$$B_k = \frac{\partial B_k}{\partial u} u. \quad (5)$$

This transverse magnetic field, constant in time but not in space, is "seen" by the ions as an rf field which acts as a time-dependent perturbation and induces sublevel transitions when the ion oscillation frequency is equal to the Larmor frequency.

For a quantitative description of this phenomenon, we consider, without loss of generality, a particle of electronic angular momentum  $J = 1/2$  and nuclear spin  $I = 0$ . In a semiclassical picture the ion is described as oscillating harmonically in the trap with frequency  $\omega$  and amplitude  $u_0$ , representing one spectral component of (2), while the interaction with the magnetic field is treated quantum mechanically. The Hamiltonian of the ion then consists of three contributions:

$$\mathbf{H} = \mathbf{H}_0 + \mathbf{H}_B + \mathbf{H}_P, \quad (6)$$

where  $\mathbf{H}_0$  is the Hamiltonian of the free ion with eigenstates  $|LSJm\rangle$ . The magnetic interaction of the particle with the longitudinal magnetic field  $B_z$  which determines the Zeeman splitting is given by  $\mathbf{H}_B$  with:

$$\mathbf{H}_B = \frac{\mu_B}{\hbar} g_J \mathbf{J}_z B_z, \quad (7)$$

while the contribution involving the transverse field  $B_k$  is described by the perturbation Hamiltonian:

$$\mathbf{H}_P(t) = \frac{\mu_B}{\hbar} g_J \mathbf{J}_k \frac{\partial B_k}{\partial u} u_0 \cos \omega t, \quad (8)$$

which, in the ion's rest frame, is a function of time.  $\mathbf{J}_i$  represents the  $i^{\text{th}}$  component of the angular momentum operator.

The time evolution of the ions under this perturbation is described by the Liouville equation:

$$\dot{\rho} = \frac{i}{\hbar} [\rho, \mathbf{H}] + \text{optical pumping}, \quad (9)$$

where  $\rho$  is the density matrix. Under our experimental conditions, excited state populations or optical coherences can be neglected, and the analysis reduces to a two-level system consisting of the ground state Zeeman sublevels  $|m = -1/2\rangle = |1\rangle$  and  $|m = +1/2\rangle = |2\rangle$ . The

interaction with the optical field contributing to optical pumping between the sublevels, can be considered as a "quasi relaxation process" resulting in a final population difference  $w^0 = \rho_{22}^0 - \rho_{11}^0$  between the states and characterized by the longitudinal and transverse time constants  $T_1$  and  $T_2$ . Depolarizing relaxations in the ground state due to collisions are neglected, as their rate is considerably smaller than the laser pumping rate  $1/T_1$ .

Under steady-state conditions, one calculates, with (6–9), a population difference

$$w = w^0 \left( 1 - \frac{\omega_R^2 T_1 T_2}{1 + \Delta\omega^2 T_2^2 + \omega_R^2 T_1 T_2} \right), \quad (10)$$

reflecting the balance of optical pumping and counter-acting sublevel transitions caused by the motion of the ions in the inhomogeneous magnetic field. Here,  $\omega_R$  is the Rabi frequency representing a measure of the transition probability between the Zeeman states due to the perturbation

$$\omega_R = \frac{\mu_B}{\hbar^2} g_J \frac{\partial B_k}{\partial u} u_0 \langle m | \mathbf{J}_k | m+1 \rangle = \frac{\mu_B}{2\hbar} g_J \frac{\partial B_k}{\partial u} u_0 \quad (11)$$

with  $g_J = 2$  and the matrix element  $\langle -1/2 | \mathbf{J}_k | 1/2 \rangle = \hbar/2$  for a spin  $1/2$  particle.  $\Delta\omega = \omega - (\omega_2 - \omega_1)$  describes the frequency detuning between the motional frequency  $\omega$  of the ions and the splitting frequency of the substates in the longitudinal field  $B_z$  given by the Larmor frequency (1) with  $\omega_2 - \omega_1 = \omega_L$ .

The population difference is minimized at resonance for  $\Delta\omega = 0$ , when the motional frequency is equivalent to the Larmor frequency. Under these conditions an atomic coherence, represented by the off-diagonal elements of the density matrix and oscillating with frequency  $\omega$ , is formed

$$\rho_{12} = -\frac{1}{2} \omega_R T_2 w^0 \frac{i + \Delta\omega T_2}{1 + \Delta\omega^2 T_2^2 + \omega_R^2 T_1 T_2} e^{i\omega t} \quad (12)$$

being maximum at resonance. We call it a self-induced coherence, because of its direct dependence on the inherent motion of the ions. As this coherence is closely related to the sublevel population changes, it can be sensitively monitored in an optical pumping experiment via optical transitions.

Excitation with  $\sigma^+$ -light at an optical transition rate  $S^+$  results in a fluorescence rate  $q = n_0 \rho_{11} S^+$ , where  $n_0$  is the number of ions in the interaction volume. Owing to a branching ratio of 2:1 for an optical decay back to state  $|1\rangle$  or state  $|2\rangle$  (Fig. 2),  $S^+$  is related to the optical pumping rate  $1/T_1$  by  $S^+ = 3/T_1$ . With  $\rho_{11} = 1 - \rho_{22} = (1 - w)/2$  and a maximum population difference  $w^0 = 1$  as the result of optical pumping at negligible relaxation between the sublevels, a fluorescence rate of

$$q = q_0 \frac{\omega_R^2 T_1 T_2}{1 + \Delta\omega^2 T_2^2 + \omega_R^2 T_1 T_2} \quad (13)$$

is found, where  $q_0 = (n_0/2)(3/T_1)$  represents the maximum observable signal at resonance and also at zero magnetic field. The resonance width is determined by the optical pumping rate and at higher sublevel transition rates is governed by "power broadening" of the line.

Since the ions are confined in a region with local variations of the transverse magnetic field, and as their oscillation amplitudes are distributed over the ion cloud, the Rabi frequency,  $\omega_R$ , varies over the cloud size, and thus modifies the lineshape of the resonance signal. The main broadening effects of a line, however, are expected to result from uncertainties in the detuning frequency  $\Delta\omega$ , for which we adduce two contributions. Thus, similar to the transverse field, the longitudinal  $B_z$  field also varies over the ion cloud and therefore causes an inhomogeneous spread in the resonance for the ions. Another contribution originates from the distribution of macro-motion frequencies over the cloud size. Such a spread results from the space charge of the cloud which flattens the pseudopotential especially in the center of the trap and makes the trap potential anharmonic. The secular frequency thus becomes dependent on the ion's position and is typically distributed over a range of several kHz [22]. Introducing a spectral distribution  $g(\omega_R, \Delta\omega)$  which represents the abundance of ions at Rabi frequency  $\omega_R$  and detuning frequency  $\Delta\omega$ , the lineshape of a motional resonance then is given by the convolution of the homogeneous and inhomogeneous contributions:

$$q(\Delta\omega) = q_0 \int \int \frac{\omega_R^2 T_1 T_2}{1 + \Delta\omega'^2 T_2^2 + \omega_R^2 T_1 T_2} \times g(\omega_R, \Delta\omega - \Delta\omega') d\omega_R d(\Delta\omega'). \quad (14)$$

The peak at zero magnetic field (z-component) is attributed to mixing of sublevel populations, caused by the precession of magnetic spin moments about a non-zero transverse field component  $B_k$  with precession frequency  $\omega_P = (\mu_B/\hbar)g_J B_k$ . As long as the field seen by an ion has a larger transverse than longitudinal component, no optical pumping can develop and increased fluorescence is observed. The sublevel population and respective fluorescence rate in the presence of a transverse and longitudinal field are found analogously to (10) and (13) by replacing  $\omega_R$  by  $\omega_P$ , and defining  $\Delta\omega$  directly as the level splitting at field strength  $B_z$  with  $\Delta\omega = \omega_L$ . The width of this peak is determined by the strength of the transverse field and the variations of the longitudinal field over the cloud size. Therefore, with some distribution  $f(\omega_P, \Delta\omega)$  representing the number of ions subjected to the fields  $B_k$  and  $B_z$ , or in frequency units  $\omega_P$  and  $\Delta\omega$  respectively, the “zero” signal can be expressed by a lineshape function similar to (14).

#### 4. Discussion of Experimental and Theoretical Results

The origin and position of the fluorescence peaks seen in Figs. 3–5, are explained well by the present theoretical model. Thus the measurements can also be used to obtain further insight into the motion and behavior of the ions in the trap. Ion oscillations have already been observed as sidebands of microwave transitions [16, 17] as well as optical transitions [10, 18]. However, their detection requires an additional rf field or in the optical case, highly monochromatic laser radiation. In contrast to this, our experiments were performed with broadband light sources and simple tuning of the applied dc

magnetic field. These measurements already provide the complete motional spectrum consisting of the macro- and micromotion as well as sidebands and higher harmonics.

It is characteristic of the measured spectra that the resonances at the secular frequency and the sidebands with the driving frequency appear saturated and achieve maximum intensity. For the single isotope measurement (Fig. 3) they approach the zero-peak height. Then, according to (14),  $\omega_R^2 T_1 T_2 > 1$ , which allows an estimate of the minimum Rabi frequency. With an optical pump rate in our experiments of typically  $1/T_1 \approx 100$  Hz, which is determined from time-resolved measurements of the fluorescence decay caused by optical pumping between substates far from any resonance, and with the assumption of equal time constants  $T_1 = T_2 = T$ ,  $\omega_R$  is found to be greater  $100 \text{ s}^{-1}$ .

The widths of the motional resonances are dominated by inhomogeneous broadening. As long as the ion oscillation amplitudes are much smaller than the cloud diameter, the ions see only a small local field variation, and therefore power broadening given by  $2\omega_R$  is negligible compared with the inhomogeneous effects. The contribution caused by the magnetic field inhomogeneity in the z-direction can be directly derived from the unsaturated component at the driving frequency  $\Omega$ , for which we evaluate a linewidth of  $5.5 \mu\text{ Tesla}$ , corresponding to a frequency width  $\delta\omega = 2\pi \times 25 \text{ kHz}$ . From this inhomogeneity and the assumption that the transverse variations have approximately the same magnitude as in longitudinal direction, we can further estimate a mean transverse field gradient of  $\partial B_k/\partial u \approx 1 \mu\text{ Tesla/mm}$  over an ion cloud diameter of  $5 \text{ mm}$ . The other contribution to the broadening of the motional resonances results from the frequency spread in the macromotion caused by the space charge of the ion cloud, as discussed before. From the resonance widths this contribution is estimated to be  $30 \text{ kHz}$ . For the measurement shown in Fig. 3 a further broadening may be attributed to the fact that the resonances originating from the motion in *r*- and *x*-direction overlap, but may not exactly coincide.

The lineshape and width of the zero-peak results almost exclusively from the scattering magnetic field about zero. Variations along the *z*-axis cause the same broadening as observed at the driving frequency  $\Omega$ , but now an additional broadening has to be assigned to the influence of the transverse field and its distribution over the ion cloud size. This contribution can be interpreted as originating from “power broadening” proportional to the local transverse field strength.

Under the conditions described above an evaluation of the oscillation amplitude and thus the kinetic energy of the ions, from the lineshape of the motional resonances, is difficult and can only give an upper limit. A more accurate analysis is possible when the optical pump rate can be further increased and the magnetic field inhomogeneities in the trap be reduced to values for which saturation of the sublevel transition does not occur. Then the peak height of a resonance is a measure of the product,  $\omega_R T$ , from which, with the known field gradient and pump rate, the motional amplitude of the ions may be derived. Applying this procedure to the peak in Fig. 3

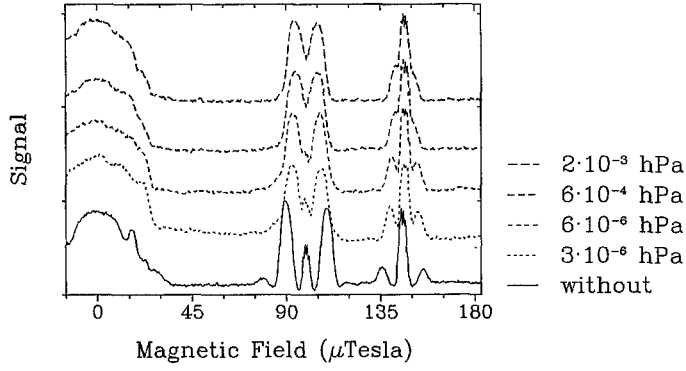


Fig. 6. Motional spectrum of  $^{173}\text{Yb}$  ions at different pressures of He buffer gas in the trap

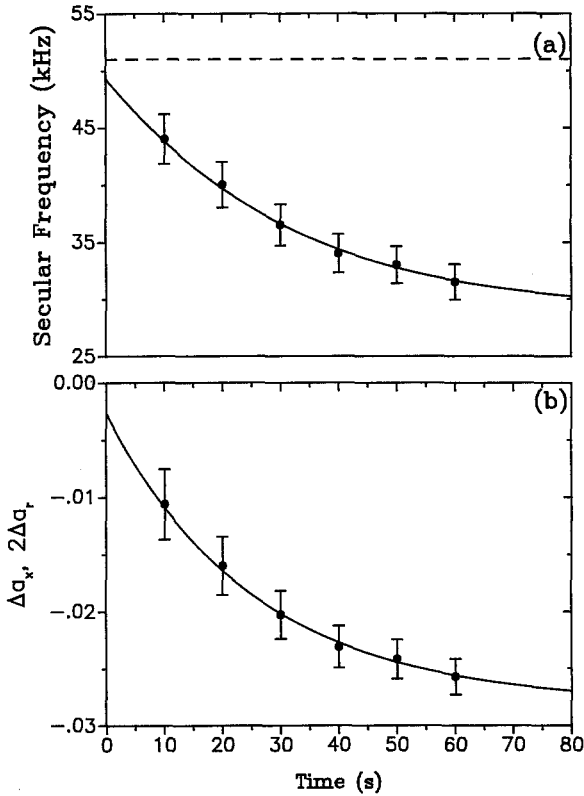


Fig. 7. a Measurement of the secular frequency of  $^{173}\text{Yb}$  and b correction parameter  $\Delta a_u$  as a function of the ion trap filling time

at  $28\ \mu\text{Tesla}$ , which is attributed to the second harmonic of  $\omega_u$ , we obtain an amplitude,  $u_0(2\omega_u)$ , for this frequency component of about  $10\ \mu\text{m}$ . From (2) this component is not expected, but it shows the deviations due to the anharmonicity of the trap potential and caused by the space charge of the ions. Therefore detailed interpretation of data derived from this kind of measurement can help to develop an improved theory applicable to big traps.

Taking advantage of the self-induced Zeeman coherences, we could observe and measure the influence of a buffer gas on the secular frequency of the ions. Figure 6 shows a series of spectra which were taken with  $^{173}\text{Yb}$  ions at different pressures of the buffer gas He. From the structure around the driving frequency,  $\Omega$ , it is found that the secular frequency,  $\omega_u$ , decreases with increasing

buffer gas pressure. The same behavior is reflected by the signal around  $140\ \mu\text{Tesla}$ , which results from sub-level transitions induced by an additionally irradiated rf field, and shows the macromotion as sidebands. In the presence of a background gas the stored ions heated by the driving field of the trap, can dispose some of their kinetic energy via collisions with the gas. This process known as cooling by buffer gases, is associated with a contraction of the ion cloud and equivalently an increase of the space charge density. Calculations taking into account the ion density [23,24], show that the effective trap potential seen by the ions is influenced by its own charge density, and in this way reacts upon the macromotion. The measurements in Fig. 6 reveal this dependence and show qualitative agreement with the calculations.

A similar detuning of the secular frequency is observed when the absolute number of ions stored in the trap is varied by stepwise increase of the ion trap filling-time (Fig. 7a). Assuming a constant ionization rate and a maximum number of ions stored in the trap, we expect the space charge to build up exponentially in time and to cause an appropriate shift of the secular frequency. This shift can be approximately accounted for by adding a space charge dependent term  $\Delta a_u$  to the  $a$ -value under the root of (3), where  $\Delta a_x = 2\Delta a_r = -8e\Delta U_{dc}/(Mr_0^2\Omega^2)$  and  $e\Delta U_{dc}$  represents the change of the potential originating from the space charge. Bearing in mind that  $\omega_u = \beta_u\Omega/2$ , we derive  $\Delta a_u = 4(\omega_{sc}^2 - \omega_u^2)/\Omega^2$ , where  $\omega_{sc}$  denotes the observed secular frequency shifted by the space charge, and  $\omega_u$  is the unshifted frequency as calculated from the trap parameters and indicated as dotted line in Fig. 7a. Thus,  $\Delta a_u$  assumes negative values and decreases exponentially with increasing time and therefore space charge. This is indicated in Fig. 7b, where the maximum shift corresponds to a space charge density of about  $10^7\ \text{ions/cm}^3$ . The offset at  $t = 0$  is in agreement with the expected value  $\Delta a_u = 0$  within the error limits of the fit.

These measurements demonstrate the feasibility of applying self-induced coherences to detailed studies of the ion motion and storage behavior in an rf trap.

## 5. Conclusion

We have presented a new method for the measurement of motional frequencies and amplitudes of stored ions in an rf trap. It was demonstrated that ions subjected to a small magnetic field undergo sublevel transitions between adjacent Zeeman states when their motional frequency is equal to the Larmor frequency in the applied magnetic field. These transitions were sensitively detected via optical transitions by taking advantage of an optical pumping scheme. The sublevel transitions could be explained as originating from the inherent motion of the ions in a slightly inhomogeneous magnetic field. Since, under these conditions, a coherent superposition of adjacent substates was found, this phenomenon was termed self-induced Zeeman coherence. A theoretical model was developed, which describes the main features of the measured spectra.

*Acknowledgements.* The ion trap was fabricated in collaboration with the I. Institut für Experimentalphysik, Universität Hamburg. We thank Prof. P.E. Toschek for his support during this work. We would also like to acknowledge the financial support of the Deutsche Forschungsgemeinschaft.

## References

1. W. Nagourney, J. Sandberg, H. Dehmelt: Phys. Rev. Lett. **56**, 2797 (1986)
2. Th. Sauter, W. Neuhauser, R. Blatt, P.E. Toschek: Phys. Rev. Lett. **57**, 1696 (1986)
3. J.C. Bergquist, R.G. Hulet, W.M. Itano, D.J. Wineland: Phys. Rev. Lett. **57**, 1699 (1986)
4. F. Diedrich, E. Peik, J.M. Chen, W. Quint, H. Walther: Phys. Rev. Lett. **59**, 2931 (1987)
5. D.J. Wineland, J.C. Bergquist, W.M. Itano, J.J. Bollinger, C.H. Manney: Phys. Rev. Lett. **59**, 2935 (1987)
6. H.G. Dehmelt: IEEE Trans. IM-**31**, 83 (1982)
7. D.J. Wineland, W.M. Itano, J.C. Bergquist, J.J. Bollinger, J.D. Prestage: In *Atomic Physics 9*, ed. by R.S. Van Dyck, Jr., E.N. Fortson (World Scientific, Singapore 1984) p. 3
8. G. Werth: IEEE Trans. IM-**34**, 238 (1985)
9. H. Knab, K.-D. Niebling, G. Werth: IEEE Trans. IM-**34**, 242 (1985)
10. J.C. Bergquist, D.J. Wineland, W.M. Itano, H. Hemmati, H.-U. Daniel, G. Leuchs: Phys. Rev. Lett. **55**, 1567 (1985)
11. J.J. Bollinger, J.D. Prestage, W.M. Itano, D.J. Wineland: Phys. Rev. Lett. **54**, 1000 (1985)
12. See, e.g., section on Trapped Ion Spectroscopy, in Proceedings of the 4th Frequency Standards and Metrology Symposium, ed. by A. De Marchi (Springer, Berlin, Heidelberg 1989)
13. R.H. Dicke: Phys. Rev. **89**, 472 (1953)
14. W. Neuhauser, H. Hohenstatt, P.E. Toschek, H. Dehmelt: Phys. Rev. Lett. **41**, 233 (1978)
15. D.J. Wineland, R.E. Drullinger, F.L. Walls: Phys. Rev. Lett. **40**, 1639 (1978)
16. H.L. Lakkaraju, H.A. Schüssler: J. Appl. Phys. **53**, 3967 (1982)
17. L.S. Cutler, R.P. Giffard, M.D. McGuire: Appl. Phys. B **36**, 137 (1985)
18. F. Diedrich, J.C. Bergquist, W.M. Itano, D.J. Wineland: Phys. Rev. Lett. **62**, 403 (1989)
19. R. Blatt, H. Schnatz, G. Werth: Phys. Rev. Lett. **48**, 1601 (1982)
20. H. Lehmitz, J. Hattendorf-Ledwoch, R. Blatt, H. Harde: Phys. Rev. Lett. **62**, 2108 (1989)
21. H.G. Dehmelt: Adv. At. Mol. Phys. **3**, 53 (1967)
22. L.S. Cutler, C.A. Flory, R.P. Giffard, M.D. McGuire: Appl. Phys. B **39**, 251 (1986)
23. E. Fischer: Z. Phys. **156**, 1 (1959)
24. F. Vedel, J. André: Phys. Rev. A **29**, 2098 (1984)